



# Strain gauges capable of measuring large cyclical deformations printed on elastic polymer films



Alexander P. Kondratov<sup>a,\*</sup>, Vladislav Yakubov<sup>b,c</sup>, Alex A. Volinsky<sup>b,\*</sup>

<sup>a</sup> Moscow Polytechnic University, ul. Bolshaya Semenovskaya, 38, Moscow 107023, Russian Federation

<sup>b</sup> Department of Mechanical Engineering, University of South Florida, Tampa, FL 33620, USA

<sup>c</sup> School of Mechanical and Manufacturing Engineering, University of New South Wales Sydney, Sydney, NSW 2052, Australia

## ARTICLE INFO

### Article history:

Received 16 January 2020

Received in revised form 7 June 2020

Accepted 9 June 2020

Available online 18 June 2020

### Keywords:

Strain gauge

Automatic feeding

Polymeric films

Hard elastic polypropylene

Crazing

Electrical conductivity

Adhesion

## ABSTRACT

A process is presented for screen printing of an electrically conductive coating on elastic polymer films to produce strain gauges capable of measuring large reversible deformations, suitable for use in the medical industry or for the next generation of industrial robots. The manufacturing process includes cyclical deformation of the film, film stretching before printing, and film stretching during conductive liquid application. Film stretching by specialized printing equipment and application of electrically conductive liquid are described, and performance comparison of strain gauges is provided.

© 2020 Published by Elsevier Ltd.

## 1. Introduction

Sensors that change electrical resistance with deformation (strain gauges) are some of the most common types of printed electronic devices mass-produced by high-capacity manufacturing equipment [1–5]. Flexible strain gauges printed on paper, polymer films, and non-woven or woven fabric are used for monitoring the movement of industrial robots, testing and operating mechanical devices for various purposes, and to monitor the human musculoskeletal system [2–5]. Strain gauges work on the principle of change in electrical resistance of wire or metal foil during tensile strain application.

The maximum deformation limit of commercially produced strain gauges using wire or metal foil is 2–10% [3,4]. Large deformations over 100% are measured by mercury-containing liquid metal sensors, which produce a non-linear response to tensile strain [6]. Therefore, the use of strain gauges in sports, the medical industry, and the field of soft robotics or wearable electronics is prohibited or significantly limited.

Strain gauges are developed for specific applications and are operated by altering the strain gauge dimensions, the electrically

conductive element layer dimensions, the composition of the electrically conductive element, the composition and structure of the substrate, and the method of connecting the substrate to the electrically conductive element.

For strain gauge manufacturing, various methods are used to connect the electrically conductive element with the substrate, such as focused ion beam milling [7], electrospinning [8], injection [9], and sputtering [10], which impose significant limitations on manufacturability. Of the research on printed strain gauges production, particular interest has been placed on sensors for monitoring the movement of the human body [6,11], requiring measurement of tensile strain up to 60% [12]. Currently, strain gauges for this application are made by applying an L-shaped pre-stretched element cut out of electrically conductive fabric onto a silicone substrate, followed by the deposition of silver using a screen-printing method. A distinctive feature of this sensor is the possibility of measuring not only tension and compression, but also pressure and bending.

Min et al. [13] presented a more advanced production method of strain gauges by directly applying silver nanoparticles and multi-walled carbon nanotubes in an aerosol form onto elastic polydimethylsiloxane film. These sensors measure tensile strain up to 74%. However, aerosol printing is problematic due to significant splashing of droplets during aerosol application and the coffee ring effect due to uneven evaporation of the solvent [13], and

\* Corresponding authors.

E-mail addresses: [a.p.kondratov@mospolytech.ru](mailto:a.p.kondratov@mospolytech.ru) (A.P. Kondratov), [volinsky@usf.edu](mailto:volinsky@usf.edu) (A.A. Volinsky).

the electrostatic repulsion of falling droplets near the surface of target material [14]. This uneven distribution of conductive material can lead to the strain gauge elements being connected improperly, which will result in an incorrect response when the sensor is deformed. Application of conductive liquid is better controlled with inkjet printing. However, the use of capillary action limits this method in terms of layer thickness, uniformity, and spatial resolution of elements [15]. A comparison of technologies and potential usability of screen printing and inkjet printing to produce strain gauges for various purposes are given in references [16,17].

The main problems of strain gauges produced via both methods are irreversible mechanical separation of conductive particles in the electrically conductive layer leading to an open electrical circuit [11,13,16,18], deviations of the shape and dimensions of the conductive elements from the intended form [19], high coefficient of thermal expansion of metals used as fillers in the electrically conductive liquid [20], and low adhesion of the conductive layer to the elastic polymer substrate. These problems can be partially solved by introducing additional components to the electrically conductive liquid that increase adhesion [15,19], utilizing conductive particles with different properties [7,11,13], pre-stretching the substrate material [17,19], and additional post-printing heat treatment to remove dielectric layers between conductive particles [18].

In our previous work [19], polymer substrate strain gauges capable of measuring large deformations were produced without the need for complicated processes traditionally necessary for adhesion of the electrically conductive element with the substrate. However, the stretching and contraction of the polypropylene film were performed using a tensile testing machine. Therefore, it was not possible to realize immediate film contraction, which is favourable for the mechanical capture of the conductive liquid. The goal of this work is to study the possibility of enhancing the adhesion of the electrically conductive layer to the elastic polymer substrate and create a device for this new printing process. This requires the design of a new machine specialized for this purpose. The machine must elastically stretch a polymer film sheet cyclically, normalize the stretch before the film is fed into a printing device, and instantly contract the film after the conductive layer is applied.

## 2. Materials and methods

### 2.1. Materials

Sun Chemical Graphite Ink 26-8203 was used as the conductive printing liquid. Two types of polypropylene materials with different structure and physical–mechanical characteristics were used as a substrate for strain gauges:

- Hard elastic polypropylene films (HEPP), isotactic polypropylene Caplen 020, 30  $\mu\text{m}$  thick.
- Needle-punched cloth made of polypropylene fibers (NWPP) with 160  $\text{g}/\text{cm}^2$  mass per unit area.

When these materials are elastically deformed under tension, the crystalline structure of rigid-elastic films becomes reversibly microporous. This is known as the dry crazing effect and is manifested in a cyclical change in the color of films in polarized light [21]. The microporosity of films reaches a maximum with a relative elongation of 20% [19].

HEPP test films were subjected to cyclical stretching and contraction using a tensile machine with a constant lower grip speed of 3 mm/s and an amplitude of change in relative deformation of 2–160% (Fig. 1). The NWPP material was not subjected to this test.

According to the data shown in Fig. 1, the HEPP film is elastic and has practically no permanent deformation. By observing cyclical film stretching and contraction at a speed of 3 mm/s, it is established that the film contracts with a speed of at least 3 mm/s, and the sample does not sag.

### 2.2. Strain gauge and printing platform design

To study the mechanical and electrical parameters of proposed strain gauges and to test the printing process, three types of electrically conductive elements, differing in length, were used (Fig. 2).

To obtain strain gauges printed on polypropylene film, a stretching platform was designed and manufactured. This device stretches a polypropylene film sheet a single time or multiple times in the air before printing and a single time when conductive liquid is applied to the film. Stretching can be carried out to various degrees of film elongation by lowering a lever and adjusted by

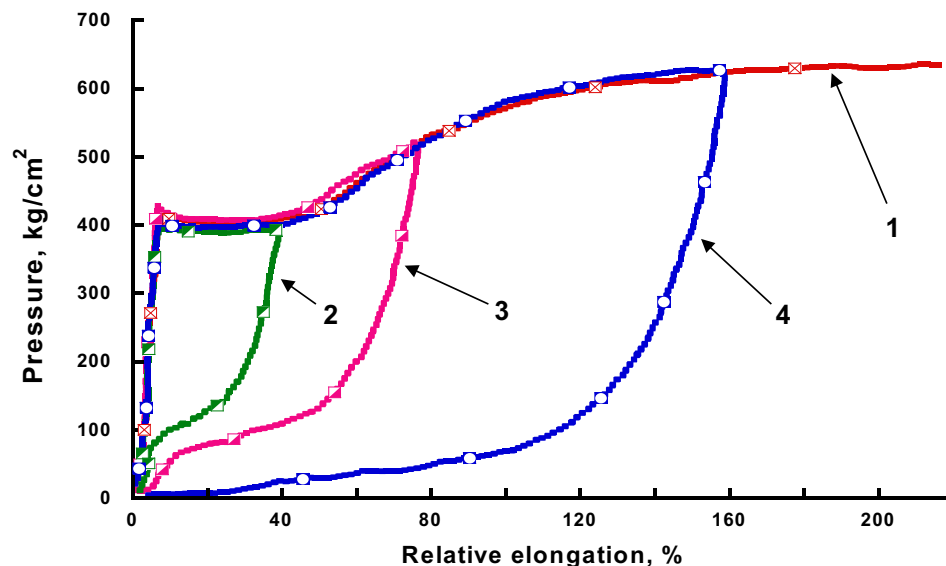


Fig. 1. Initial stretching and contraction cycles of the HEPP polypropylene film: 1 – stretching to failure; 2, 3, 4 – stretching to relative elongation of 40%, 80%, and 160% with contraction to the original length.

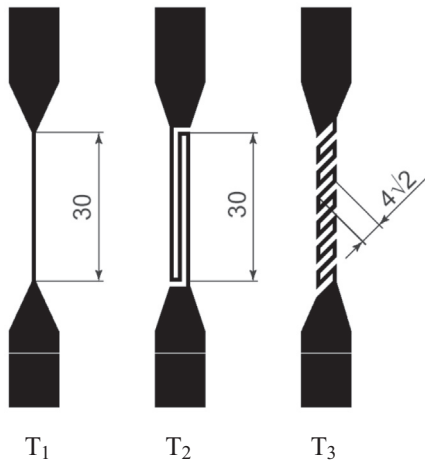


Fig. 2. The shape and size of printed strain gauges. The length is in millimeters.

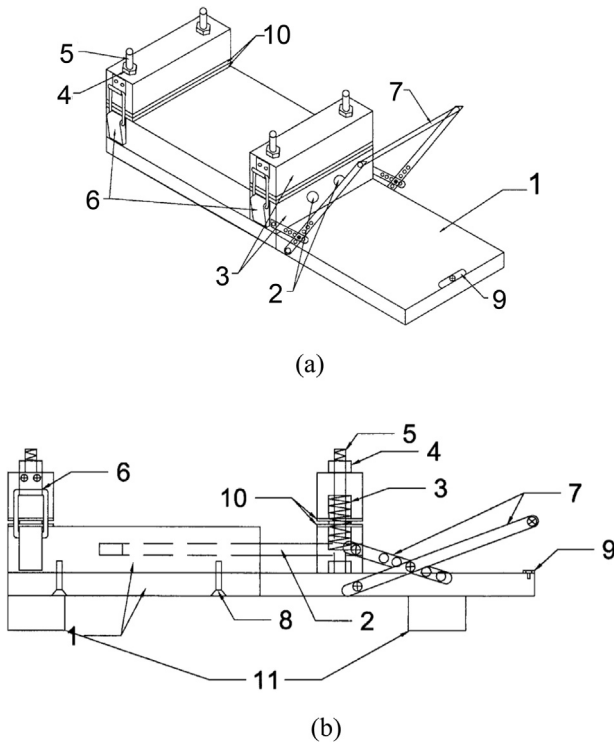


Fig. 3. The crank-slider mechanism of the stretching platform. (a) isometric view, (b) side view. Here, 1 – platform base; 2 – sliding guides; 3 – spring return; 4 – nut; 5 – a bolt; 6 – latch for fixing the film clip; 7 – lever; 8 – connecting bolts; 9 – lever position lock; 10 – rubber cloth; 11 – platform supports.

changing the lengths of the machine components. An isometric view and a side view of the stretching platform layout are shown in Fig. 3(a,b).

To calculate and program film stretching using the stretching platform, a kinematic diagram of the crank-slider mechanism is used, which is shown schematically in Fig. 4(a,b).

The stretched length ( $P = A_1 - A_0$ ) of the polypropylene sheet is determined by the angle of inclination ( $\varphi$ ) and the length of levers C and B of the crank-slider mechanism as described by Eq. (1). Levers are illustrated in Fig. 4(a,b).

$$P = B * \sqrt{1 - \left(\frac{C * \sin\varphi - D}{B}\right)^2} - C * \cos\varphi \quad (1)$$

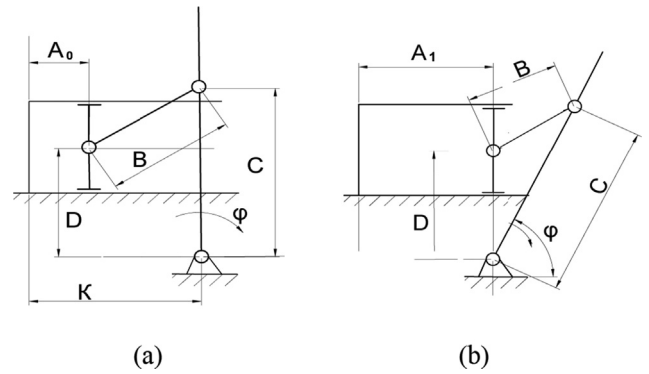


Fig. 4. Kinematic diagram of the crank-slider mechanism for calculating the deformation of the film on the stretching platform: (a) before and after the printing phase; (b) position during printing.

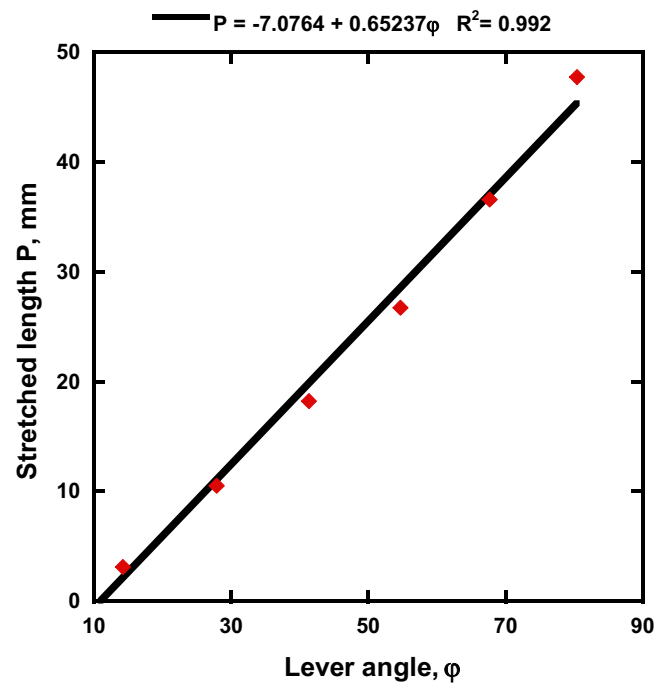


Fig. 5. Change in film deformation with the inclination angle  $\varphi$  of the lever C on the stretching platform. Lever length is constant with  $C = 45$  mm,  $B = 50$  mm, and  $D = 25$  mm.

Here, A is the length of the film, B and C are the lengths of levers B and C, D is the distance from the middle of the slider to the hinge support, and  $\varphi$  is the angle of inclination of lever C. In this case, deformation  $\varepsilon$  is equal to:

$$\varepsilon = \frac{A_1 - A_0}{A_0} \quad (2)$$

Stretched film length can be approximated using the linear equation shown in Fig. 5.

To ensure constant and accurate film strain with increased printing speed, it is important to securely fix the angle of the lever C. If it is necessary to increase or decrease the strain, lengths  $B_x$  and  $C_x$ , shown in Fig. 6, should be changed by moving the studs to different holes. To demonstrate this possibility, the nodes of the platform's lever system are denoted with additional letters L, F, K, B, E, W, and C.

The length A is found as  $A = K_x - P$ , where  $K_x$  is a constant value determined by the equipment setup.  $B_x$  is the length of the lever used during equipment setup.

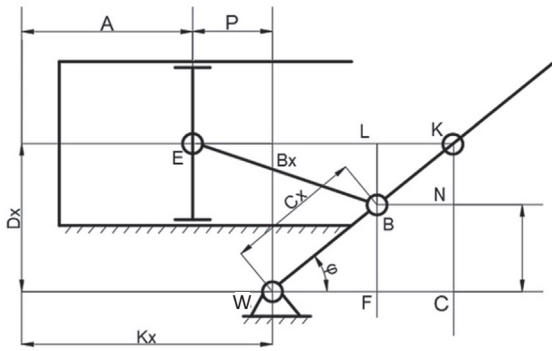


Fig. 6. Kinematic diagram of the crank-slider mechanism for calculating printing platform film strain. An explanation of the symbols is given in the text below.

$$P = EL - WF;$$

$$EL = \sqrt{B_x^2 - BL^2}A = K \pm P$$

$BL = D_x - BF$ ;  $D_x$  is a constant determined by the equipment setup;  
 $BF = C_x \sin \varphi$ ;  $WF = C_x \cos \varphi$ .

Therefore, by moving point B along the lever WK, length  $C_x$  is changed, which changes the degree of film stretching.

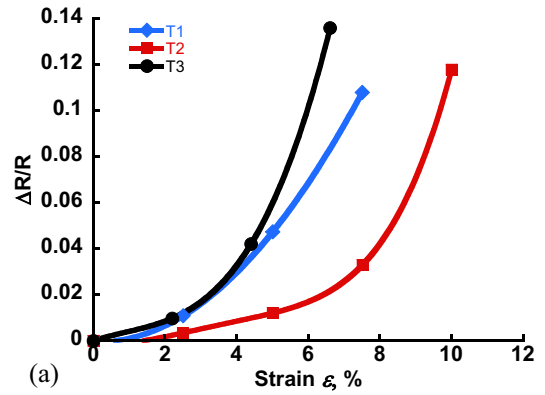
2.3. Manufacturing of strain gauges

This new method of printing strain gauges on polymer films introduces three additional operations to increase the adhesion of the electrically conductive layer to the elastic substrate. The first operation is the stretching and contraction of a hard-elastic polymer film in a gaseous medium (in the air). With this operation, a structure with open pores is formed. The second operation is the re-stretching of the film and its fixation in a stretched state, within the printing machine and under a stencil form. The third operation involves releasing the stretch so that the film immediately contracts after the conductive liquid is applied. At this stage, a conductive liquid is introduced onto the film under the action of atmospheric pressure (vacuum in the pores) and the liquid is captured by closing pores when the film is returned to an unstretched state.

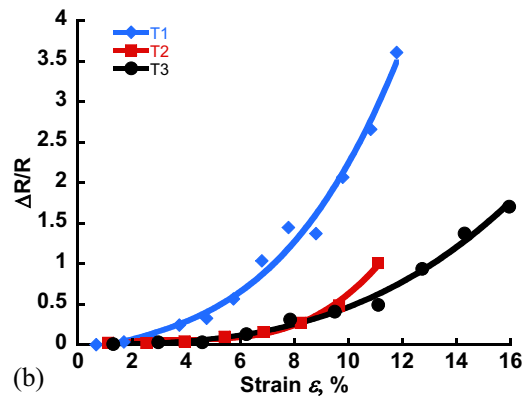
This process achieves a similar measurement range as strain gauges manufactured by the fabrication of electrically conductive composite fibers as described in [25,29]. However, the presented process requires only a commercially available polypropylene film, a stretching platform, and conductive ink. The process can be automated for mass-production.

2.4. Testing methods

Electrical and mechanical characteristics of strain gauges produced using film stretching and screen printing of electrically conductive elements are shown in Figs. 7–9. In order to show uncertainty in reported measurements, error bars for resistance measurement were determined experimentally. Ten identical sensors were made by screen printing using newly designed stretching equipment (Fig. 3). For each sample set, a different shape of the electrically conductive element (Fig. 2) was used. The current–voltage characteristics of the samples were measured with current varying between 5 mA and 100 mA, and the resistance of the sensors was therefore determined. Then, the resistance of the sensors with deformation varying from 0 to 70% was recorded, and the average values of electrical resistance of the sensors and the stan-



(a)



(b)

Fig. 7. (a) HEPP and (b) NWPP strain gauges under tensile strain with different element configurations. T1, T2, and T3 refer to strain gauge conductive element geometry shown in Fig. 2.

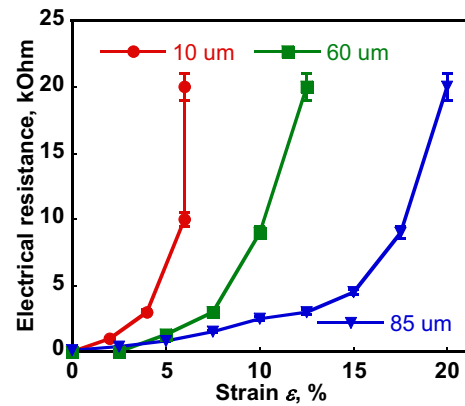
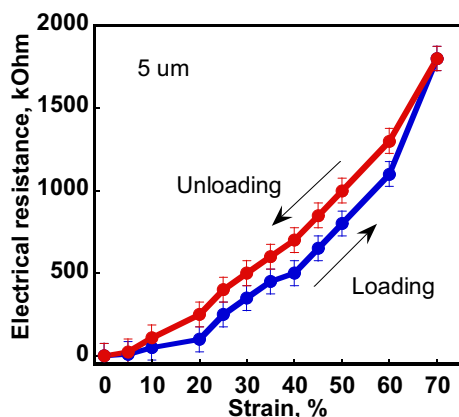


Fig. 8. The electrical resistance of printed strain gauges on nonwoven fabric (NWPP). The thickness of the electrically conductive layers is 10 μm, 60 μm, and 85 μm.

Standard deviation of the measured values, reflected by vertical lines in Figs. 8 and 9, were calculated.

2.5. Strain gauge characterization

As seen in Fig. 7, the usable range and sensitivity of the strain gauges can be adjusted by changing the configuration of the electrically conductive elements. The largest recorded value of ultimate strain for NWPP substrates is achieved using an element with a short, linear configuration, while the smallest recorded



**Fig. 9.** The electrical resistance of the strain gauge obtained by spraying a 5  $\mu\text{m}$  conductive paint layer onto a 50 mm thick stretched HEPP film.

value of ultimate strain is achieved using a long, zigzag configuration (Fig. 7b). For the HEPP film substrates, the opposite was observed, with the zigzag configuration capable of recording the highest strain (Fig. 7a).

The electrical resistance of the strain gauges depends on the thickness of the conductive layer (Fig. 8). The thickness of the layer is adjusted by changing the gridline mesh used in screen printing. When the thickness of the conductive layer is 10  $\mu\text{m}$ , the linear strain measurement range is 0–3%. When the thickness of the conductive layer is 60  $\mu\text{m}$ , the linear range of strain measurement is 0–8%. When the thickness of the conductive layer is 85  $\mu\text{m}$ , the linear range of the strain measurement is 0–18%. Printed strain gauges can be used as mechanical switches or open circuit sensors by programming a specific resistance into an electrical circuit and choosing the appropriate conductive layer thickness. A threshold resistance of 20 k $\Omega$  is achieved at 5%, 13%, and 20% elongation with 10  $\mu\text{m}$ , 60  $\mu\text{m}$ , and 85  $\mu\text{m}$  layer thickness, respectively. Strain gauges capable of measuring tensile strain over 70% can be manufactured using the proposed machine (Fig. 4), where the initial stretching of the film substrate is determined by kinematic parameters of the crank-slider mechanism. This requires a new method of applying the electrically conductive liquid to the stretched film and the use of liquids with low viscosity.

Fig. 9 shows the change in electrical resistance of the printed strain gauge with the tensile strain. The relative tensile strain measurement range is 0–70%. The difference in strain gauge resistance between the stretching and contraction phases for equal strain does not exceed measurement error. As can be seen, the 500 k $\Omega$  resistance corresponds to a strain of nearly 40% during loading and 30% during unloading. Therefore, the error in measuring strain in this range is  $\pm 5\%$ .

The stability of strain gauge performance during large cyclic deformation is a result of polymer substrate peculiarities and the conductive layer adhesion mechanism. During stretching, crazing occurs on the polypropylene film surface, resulting in the formation of nanopores and micropores [22]. Crazing initiates on the first stretching operation. The high specific energy of the craze morphology decreases during conductive liquid application due to the adsorption of liquid surfactant. Instant contraction of the film after contact with conductive liquid allows the liquid to be mechanically captured, which fills the substrate pores with electrically conductive particles. After pores shrink and the solvent is pressed out due to film contraction [23], electrically conductive particles are concentrated on the film surface and are in contact within the film, producing strain gauges with high electrical conductivity and large cyclical deformation capability.

**Table 1**

Comparison of gauge factors, tested strains, and sensor materials for strain gauges.

Sensor material	Gauge factor	Max. tested strain (%)	Ref.
Silver nanoparticle ink	3 (3–10% $\epsilon$ )	270*	[24]
Silver coated polystyrene/PDMS	27.6 (0–60% $\epsilon$ )	140*	[25]
Graphene nanoplatelets/NCYR/PDMS	4.5 (15–150% $\epsilon$ )*	150	[26]
Graphite oxide/PVDF	14.5 (0–15% $\epsilon$ )	16*	[27]
MWCNT/PVA	0.7 (2–10% $\epsilon$ )	10	[28]
Silver nanowires/PDMS	0.7 (0–50% $\epsilon$ )	50	[29]
Graphite ink	23.3 (20–70% $\epsilon$ )	70	This work

\* Estimated from a graph.

Table 1 compares the characteristics of strain gauges in this work with others capable of measuring large deformations. As can be seen, strain gauges manufactured using our methods provide a high gauge factor and a large range of measurable strain. To calculate the gauge factor, data for the HEPP film with a 5  $\mu\text{m}$  conductive layer were used. The nominal resistance and elongation values were taken at 20% strain instead of the unstrained state, and only the 20–70% strain range was considered. This is necessary because the resistance of the unstrained sensor is near zero for this particular sensor configuration, leading to an extremely high gauge factor when this point was used for calculation. To compensate for nonlinearity, the gauge factor was found individually for each available 20–70% strain range data point. These data were then used to calculate the average gauge factor, listed in Table 1.

### 3. Conclusions

A new method and machine are proposed for screen printing strain gauges on hard-elastic polypropylene films, allowing for measurement of tensile deformation up to 70%. The amplitude of film stretching during printing is adjusted by changing the rotational angle of the lever and/or the length of the crank-slider elements. A comparative performance assessment of strain gauges of various shapes printed on polymer films by applying graphite in a liquid form is presented.

### Funding

This work was carried out with the financial support of the Ministry of Science and Higher Education of the Russian Federation (State assignment “Structure and properties of polymer materials obtained with the use of systems of methods of chemically, thermally and/or mechanically induced surface and volume modification”, topic number FZRR-2020-0024, code 0699-2020-0024). AAV and VY acknowledge support from the National Science Foundation (IRES 1358088).

### Credit authorship contribution statement

**Alexander P. Kondratov:** Conceptualization, Methodology, Validation, Investigation, Data curation, Resources, Writing - original draft. **Vladislav Yakubov:** Methodology, Formal analysis, Data curation, Writing - original draft, Writing - review & editing, Visualization. **Alex A. Volinsky:** Formal analysis, Writing - review & editing, Visualization, Supervision.

### Declaration of competing interest

The authors declare that they have no known competing financial interests or personal relationships that could have appeared to influence the work reported in this paper.



## References

- [1] M. Borghetti, M. Serpelloni, E. Sardini, S. Pandini, Mechanical behavior of strain sensors based on PEDOT:PSS and silver nanoparticles inks deposited on polymer substrate by inkjet printing, *Sens. Actuators, A* 243 (2016) 71–80.
- [2] Y. Lu, M.C. Biswas, Z. Gu, J.W. Jeon, E.K. Wujcik, Recent developments in bio-monitoring via advanced polymer nanocomposite-based wearable strain sensors, *Biosens. Bioelectron.* 123 (2018) 167–177.
- [3] G.Y. Lee, M.S. Kim, H.S. Yoon, J. Yang, J.B. Ihn, S.H. Ahn, Direct printing of strain sensors via nanoparticle printer for the applications to composite structural health monitoring, *Procedia CIRP* 66 (2017) 238–242.
- [4] Y.H. Kwak, W. Kim, K.B. Park, K. Kim, S. Seo, Flexible heartbeat sensor for wearable device, *Biosens. Bioelectron.* 94 (2017) 250–255.
- [5] H. Wang, Y. Tong, X. Zhao, Q. Tang, Y. Liu, Flexible, high-sensitive, and wearable strain sensor based on organic crystal for human motion detection, *Org. Electron.* 61 (2018) 304–311.
- [6] V.A. Mecheda, *Tenzometricheskii metod izmereniya deformatsiy*, Samara State Aerospace University Publishing, 2011, ISBN 978-5-7883-0838-8.
- [7] Y. Quan, M.S. Kim, Y. Kim, S.H. Ahn, Colour-tunable 50% strain sensor using surface-nanopatterning of soft materials via nanoimprinting with focused ion beam milling process, *CIRP Ann.* 68 (2019) 595–598.
- [8] M. Ren, Y. Zhou, Y. Wang, G. Zheng, K. Dai, C. Liu, C. Shen, Highly stretchable and durable strain sensor based on carbon nanotubes decorated thermoplastic polyurethane fibrous network with aligned wave-like structure, *Chem. Eng. J.* 360 (2018) 762–777.
- [9] W. Hou, N. Sheng, X. Zhang, Zh. Luan, P. Qi, M. Lin, Y. Tan, Y. Xia, Y. Li, K. Sui, Design of injectable agar/NaCl/polyacrylamide ionic hydrogels for high performance strain sensors, *Carbohydr. Polym.* 211 (2019) 322–328.
- [10] D.M. Chun, S.H. Ahn, Deposition mechanism of dry sprayed ceramic particles at room temperature using a nano-particle deposition system, *Acta Mater.* 59 (2011) 2693–2703.
- [11] Y.S. Rim, S.H. Bae, H. Chen, N. De Marco, Y. Yang, Recent progress in materials and devices toward printable and flexible sensors, *Adv. Mater.* 28 (2016) 4415–4440.
- [12] J. Tolvanen, J. Hannuand, H. Jantunen, Stretchable and washable strain sensor based on cracking structure for human motion monitoring, *Nature Scientific Reports* 8 (2018) 13241.
- [13] S.H. Min, G.Y. Lee, S.H. Ahn, Direct printing of highly sensitive, stretchable, and durable strain sensor based on silver nanoparticles/multi-walled carbon nanotubes composites, *Compos. B Eng.* 161 (2019) 395–401.
- [14] A.P. Kondratov, M.A. Savel'ev, Dynamics of the remote and contact interaction of liquid droplets with film-like and fibrous-porous polymeric materials, *Russ. J. Gen. Chem.* 88 (2018) 2740–2746.
- [15] G. Hassan, J. Bae, A. Hassan, Sh. Ali, Ch.H. Lee, Y. Choi, Ink-jet printed stretchable strain sensor based on graphene/ZnO composite on micro-random ridged PDMS substrate, *Compos. A Appl. Sci. Manuf.* 107 (2018) 519–528.
- [16] Y. Zhang, N. Anderson, S. Bland, S. Nutt, G. Jursich, S. Joshi, All-printed strain sensors: building blocks of the aircraft structural health monitoring system, *Sens. Actuators, A* 253 (2017) 165–172.
- [17] A.P. Kondratov, A.M. Zueva, I.V. Nagornova, Parameters dynamics estimation method for printed electronics conductive elements layers, in: 11th International IEEE Scientific and Technical Conference “Dynamics of Systems, Mechanisms and Machines”, Dynamics 2017 – Proceedings.
- [18] I.V. Nagornova, E.B. Bablyuk, O.V. Lazareva, O.V. Trapeznikova, E.B. Charushina, Algorithmic presentation of printed electronics verification in-process, *J. Phys.: Conf. Ser.*, 1260 (2019).
- [19] A.P. Kondratov, A.M. Zueva, R.S. Varakin, I.P. Taranec, I.A. Savenkova, Polymer film strain gauges for measuring large elongations, *IOP Conference Series: Materials Science and Engineering*, C (2018), .012013
- [20] A.P. Kondratov, G.M. Zachinjev, Thermal cyclic tests of shrink polymeric products with the shape memory, in: Proceedings of the 2015 International Conference on Testing and Measurement: Techniques and Applications, C (2015), pp. 73–76.
- [21] A.P. Kondratov, New materials for light strain-optical panels, *Light & Engineering Svetotekhnika* 22 (2014) 74–77.
- [22] L.G. Varepo, I.N. Ermakova, I.V. Nagornova, A.P. Kondratov, Diagnostics of transparent polymer coatings of metal items, *AIP Conf. Proc.* 1876 (2017) 020080, <https://doi.org/10.1063/1.4998900>, American Institute of Physics.
- [23] E.S. Trofimchuk, A.V. Efimov, N.I. Nikonorova, A.L. Volynskii, N.F. Bakeev, L.N. Nikitin, A.R. Khokhlov, L.A. Ozerina, Crazing of isotactic polypropylene in the medium of supercritical carbon dioxide, *Polym. Sci. Ser. A* 7 (2011) 546–557.
- [24] J.C. Yeo, H.K. Yap, W. Xi, Z.P. Wang, C.H. Yeow, C.T. Lim, Flexible and stretchable strain sensing actuator for wearable soft robotic applications, *Adv. Mater. Technol.*, 1 (2016), Article 1600018.
- [25] Y.G. Hu, T. Zhao, P.L. Zhu, Y. Zhang, X.W. Liang, R. Sun, C.P. Wong, A low-cost, printable, and stretchable strain sensor based on highly conductive elastic composites with tunable sensitivity for human motion monitoring, *Nano Res.* 11 (2018) 1938–1955.
- [26] J.J. Park, W.J. Hyun, S.C. Mun, Y.T. Park, O.O. Park, Highly stretchable and wearable graphene strain sensors with controllable sensitivity for human motion monitoring, *ACS Appl. Mater. Interfaces* 7 (2015) 6317–6324.
- [27] M.C. Zhang, C.Y. Wang, Q. Wang, M.Q. Jian, Y.Y. Zhang, Sheath-core graphite/silk fiber made by dry-meyer-rod-coating for wearable strain sensors, *ACS Appl. Mater. Interfaces* 8 (2016) 20894–20899.
- [28] B.F. Gonçalves, J. Oliveira, P. Costa, V. Correia, P. Martins, G. Botelho, S. Lanceros-Mendez, Development of water-based printable piezoresistive sensors for large strain applications, *Compos. B Eng.* 112 (2017) 344–352.
- [29] S. Yao, Y. Zhu, Wearable multifunctional sensors using printed stretchable conductors made of silver nanowires, *Nanoscale* 6 (2014) 2345–2352.